Proceedings of the 11th International Coral Reef Symposium, Ft. Lauderdale, Florida, 7-11 July 2008
Session number 17

Pre-Processing 2005 AVIRIS Data for Coral Reef Analysis

B. Lobitz[1], L. Guild[2], R. Armstrong[3], M. Montes[4], J. Goodman[3]

1) University Corporation at Monterey Bay, MS242-4, NASA Ames Research Center, Moffett Field, CA 94035
2) NASA, MS242-4, NASA Ames Research Center, Moffett Field, CA 94035
3) University of Puerto Rico at Mayagüez, Mayagüez, PR 00681
4) Naval Research Laboratory, Code 7232, Washington, DC 20375

Abstract. In December 2005, the Airborne Visible Infrared Imaging Spectrometer (AVIRIS) was flown over Puerto Rico and the U.S. Virgin Islands for assessment of the 2005 Caribbean coral reef bleaching event. The resulting hyperspectral imagery is being used as the foundation for evaluating coral distribution and health in these areas. Image processing for this analysis consisted of an important pre-processing phase, followed by a spectral-based benthic classification phase. A critical aspect of the pre-processing was correcting for an adverse stray-light anomaly present in the imagery. The anomaly is characterized by higher than expected radiance values near the center of each flight line accompanied by a small decay of radiance values near the left edge of each flight line. The anomaly is present in AVIRIS imagery acquired from 2004-2006 and is most noticeable over water features in the near-infrared channels. We present an overview of the entire pre-processing phase, including suppression of the stray light anomaly and the edge decay, as well as sun glint removal and atmospheric correction.

Key words: AVIRIS, stray light, sun glint, atmospheric correction

Introduction

Spectral information from corals and other associated habitat components can be detected through a clear shallow water column using remote sensing instruments. Spectral discrimination of reef bottom types (i.e., coral, algae, and carbonate sand) is possible using field spectroscopy methods (Hochberg and Atkinson 2000; Hochberg et al. 2003) as well as using spectral image analysis techniques (Goodman and Ustin 2007; Hedley and Mumby 2003; Mobley et al. 2005). However, only visible light penetrates deeply into the water column, water properties are typically variable, and the benthic surface is spatially heterogeneous. Thus, due to the spectral complexity of this environment, data from imaging spectrometers with multiple spectral channels in the visible portion of the electromagnetic spectrum, such as the Airborne Visible Infrared Imaging Spectrometer (AVIRIS), can potentially provide better maps of benthic types, compared to multispectral sensors.

Analysis of benthic composition using remote sensing requires a number of pre-processing steps to convert the measured at-sensor radiance into reflectance data. This is because at-sensor radiance represents a complex combination of absorption and scattering features from the atmosphere, spectral interactions at the air-water interface, absorption and scattering from the water column and reflectance from the benthic surface. The sensor system itself can also add artifacts and noise during the recording process. As an important first step in effective image analysis, pre-processing is utilized to remove the confounding effects of sensor artifacts, atmospheric influence, and specular reflection from the water surface (i.e., sun glint).

We present a series of techniques utilized for pre-processing AVIRIS imagery acquired in 2005 from Puerto Rico and the U.S. Virgin Islands. Output derived from these techniques is in the format of remote sensing reflectance at the water surface, which is subsequently being used to retrieve bathymetry and water properties and to classify the benthic substrate following methods adapted from Goodman and Ustin (2007). The resulting image products are being utilized in conjunction with field surveys to assess coral distribution and health following the 2005 bleaching event (Guild et al. 2008).

Materials and methods

In mid-December 2005, AVIRIS was flown on the NASA Twin Otter over sites in SW Puerto Rico and the U.S. Virgin Islands to investigate impacts from the 2005 coral bleaching event. The Twin Otter was flown at an altitude of 3.5km, producing an image spatial resolution of approximately 3.1m. A handheld spectroradiometer (GER1500, Spectra Vista

Corporation) was concurrently used in the field to acquire reflectance measurements of the water surface at three locations.

While AVIRIS has a long history of improvements while providing high-quality imaging-spectrometer data (Green et al. 1988; Carder et al. 1993; Green et al. 1993; Sarture et al. 1995; Clark and Swayze 1996; Eastwood et al. 2000; Green and Boardman 2000; Green and Pavri 2000), in some situations the data still contain unwanted features that need to be corrected. In 2004, a new foreoptics section was installed on the system. This significantly improved the signal-to-noise ratio of the instrument (i.e., increased instrument performance), particularly in the visible portion of the spectrum, but introduced a stray-light anomaly in imagery acquired from 2004-2006. The stray light is a portion of light that has entered the instrument and should be recorded at a given measurement location (i.e., pixel), but is further reflected within the instrument, becomes mixed with other light, and subsequently inappropriately recorded at a different location. The resulting anomaly is visually apparent as a "glow" of incorrect data surrounding a stripe of "good" data where the stray-light effect is not present (Fig. 1a). Because this anomaly is a function of stray light from nearby pixels, and because land features typically reflect light strongly in near-infrared wavelengths, the anomaly is stronger at the land-water boundary and most significant in the near-infrared channels (750-1300nm). Although the anomaly is minor in the visible-wavelength channels (370-700nm) (Fig. 1b), where aquatic remote sensing is primarily focused, artifacts in the near-infrared can be transferred to the visible channels via sun glint suppression and atmospheric correction algorithms. While the impact of the stray-light effect is only a few percent of the relatively stronger signal over land, it can be as much as ~40% of the significantly lower signal over water areas adjacent to land.

Pre-processing the AVIRIS imagery for subsequent benthic analysis included suppressing impacts of the stray-light anomaly, correction of an unexplained edge decay feature, suppression of sun glint and finally atmospheric correction.

The stray-light anomaly was independently suppressed for each of the affected near-infrared channels (Fig. 1c) using an adaptive line-by-line correction that differentially adjusts the left and right sides of the image. The two sides were corrected separately because the anomaly was found to be different on each side. Correction was achieved by first using a moving window (101 along-track pixels by 30 across-track pixels) to calculate the mean of the central stripe of "good" data and the means of the "glow" adjacent to the left and right of the stripe for each line. The values for the individual pixels on each side of the image were then reduced as a function of the difference between the mean of the central stripe and the mean of the respective left or right "glow", scaled by the pixel distance from the central stripe (Fig. 2).

The decay feature along the edges of each image impacted the first seventy pixels (Fig. 3) and the last pixel in each row. This limb effect was corrected by first computing the across-track column means for a designated training area within deep water in each flight line, which was assumed to be spectrally homogenous (i.e., a flat field). Scale factors were then calculated to normalize each of the column means to a single mean for the training area. The resulting scale factors were used to adjust the values of the first seventy pixels and the last pixel of each respective flight line, thus making the edge pixels consistent with the more central pixels (Figs. 1c and 3).

Sun glint was suppressed (Fig. 1d) using a spectral normalizing procedure following the Hedley et al. (2005) variation of Hochberg et al. (2003). In this method the slope of the regression line, b, between pixel values from a NIR band (750nm) and each of the visible bands, i, is computed over a training sample containing sun glint. This slope is then used to reduce the values in each visible band at each pixel location, relative to the difference between the NIR-band minimum value within the training area, L_{NIRmin}, and the location-specific NIR value, L_{NIR}. For each band i, the output pixel value, $L'(i)$, is then:

$$L'(i) = L(i) - b(i)[L_{NIR} - L_{NIRmin}]$$

Atmospheric correction was performed using Tafkaa, an algorithm developed at the Naval Research Laboratory designed to address the confounding variables associated with performing atmospheric correction for shallow aquatic applications (Gao et al. 2000; Montes et al. 2001; Montes et al. 2003). The Tafkaa algorithm includes different aerosol options (none, continental, maritime, or urban) and a number of atmospheric gaseous absorption calculations (water vapor, carbon dioxide, ozone, nitrous oxide, carbon monoxide, methane, and oxygen). The algorithm was implemented using an option to retrieve per-pixel reflectance values based on pixel-specific solar illumination angles and AVIRIS viewing geometry, which provides a more explicit solution to the atmospheric correction calculations. Output was in the units of remote sensing reflectance at the water surface.

As a final step, the imagery was georectified using the internal geometry models (IGMs) and geographic lookup tables (GLTs) provided as standard ancillary files with the AVIRIS imagery (Fig. 4).

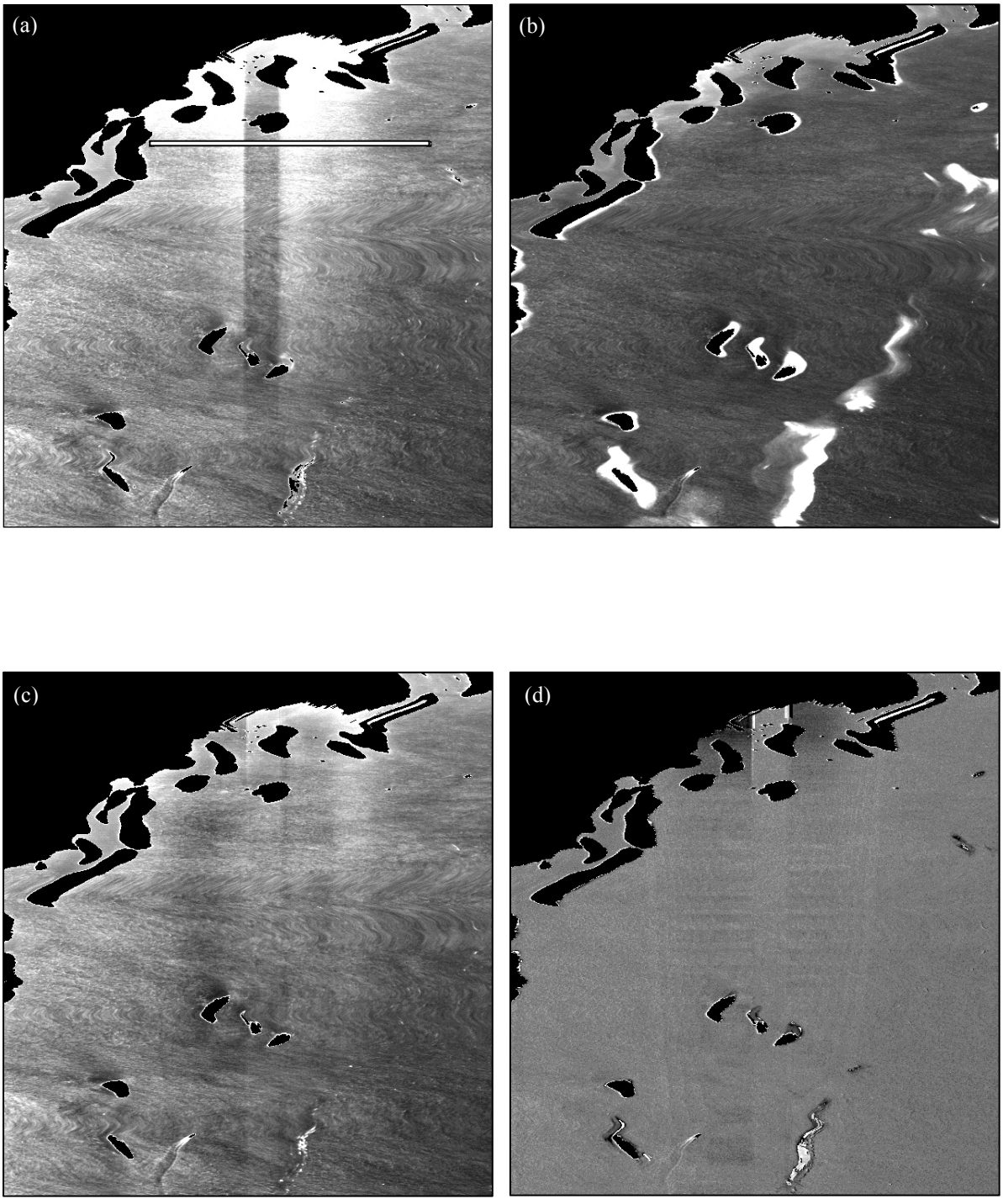

Figure 1. (a) Channel 55 (864nm, near-infrared light) within a non-georectified AVIRIS flight line subset over La Parguera, Puerto Rico. In this flight line, the stray-light anomaly was present only in the near-infrared channels. The long white box is the location of the profile shown in Fig. 3. (b) Channel 35 (672nm, visible red light). The stray-light anomaly did not affect the visible channels. (c) Channel 55 after stray-light suppression and limb correction. (d) Channel 55 after stray-light suppression, limb correction and sun glint suppression.

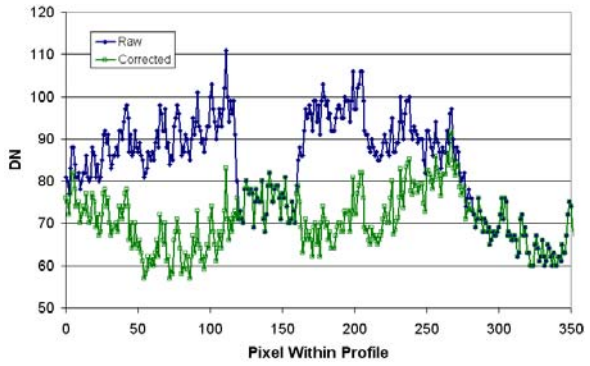

Figure 2. Cross-section profile of stray-light anomaly (from Fig. 1a). The profile shows that the digital numbers (DNs) in the relatively dark central band are similar to the background values near the edges of the swath and that the anomaly decays in magnitude away from the center of the image. The noise is due to sun glint. The corrected values were the result of adjusting the raw values to match those within the central band.

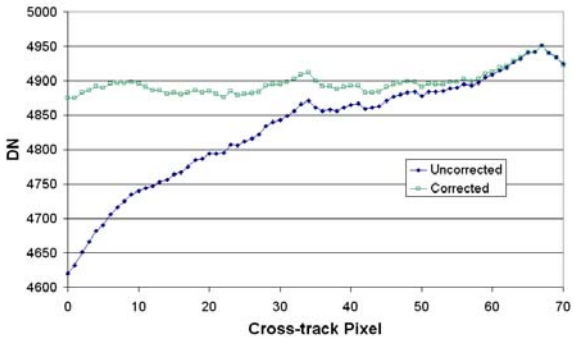

Figure 3. Deep water example of 10-channel averaged DNs within the training area (wavelengths 414-510nm) before and after limb correction. Only the first 70 pixels out of 677 are shown, demonstrating the correction on the affected side of the image.

Results

The most problematical pre-processing step was the stray-light correction, due to the variability of the effect. The magnitude of the stray-light contamination in the water depended on the proximity to land, i.e., the stray-light source, relative to the orientation of the flight line, since the amount of adjacent land determined the magnitude of the stray light. The correction estimation was further complicated by the coast line as well as the presence of patch reefs and sun glint near the coast. For the example given, Fig. 1a, and the corrected, Fig. 1c, the asymmetrical nature of the coastline and the "glow", and occurrence of small islands near the coast led to an incomplete removal of the anomaly. Generally, the post-correction values adjacent to the central stripe matched at the boundary and merged well to the magnitude of the background values (Fig. 2).

Limb corrections resulted in flatter cross-track profiles at the flight line edges (e.g., Fig. 3), which are expected for regions within the imagery that contain only water, i.e., the data are more correct. Also, this improvement should produce better mosaics when the flight lines are stitched together.

Suppressing the sun glint prior to the stray-light and limb corrections was not possible because much of the area with the stray-light contribution would have been considered glint, when the spurious values were due to a separate cause. Ideally, the sun-glint and atmospheric corrections should be performed concurrently, because they affect each other, but incorporating the atmospheric correction processing into the sun-glint suppression program was not possible.

Once all the pre-processing steps on the AVIRIS data were completed (Fig. 1) and the imagery was georectified (Fig. 4), image spectra were extracted from three locations where surface reflectance was measured concurrently in the field (Fig. 5). The AVIRIS-derived reflectance values were somewhat low compared to the field data for all three of the field sites at that location, but generally indicated good agreement between the image data and field measurements. More field data of water-leaving reflectance measurements from other locations would have allowed for better comparisons of the AVIRIS data to field conditions, but with limited equipment and a primary focus on collecting benthic reflectance measurements for habitat mapping, only limited data were available for the water surface.

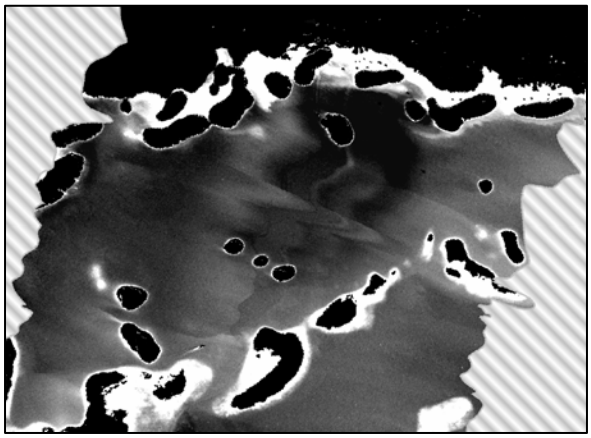

Figure 4. Channel 35 (672nm, red light) subset of sample image following complete pre-processing scheme. The wavy edges are an artifact of, primarily, the roll correction.

Discussion

As a research instrument, AVIRIS has undergone numerous changes and improvements over the years. The foreoptics section change implemented in 2004 improved overall sensor performance, but resulted in an unfortunate stray-light anomaly (note the stray-light anomaly was fixed for the 2007 flight season and only impacted data in the 2004-2006 seasons).

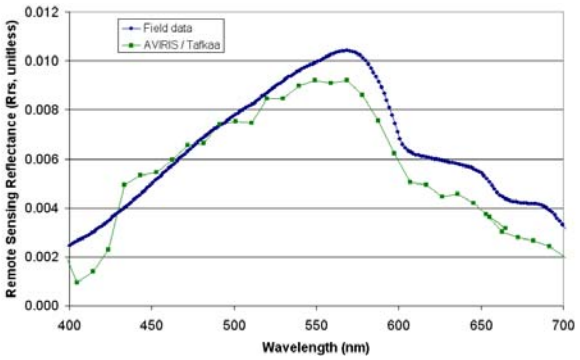

Figure 5. Image-derived and field-measured, remote sensing reflectance (R_{rs}) for one of three near-shore water sites. On average, the image-derived values were 16% lower than the field data.

We have presented an overview of the methodology used for correcting this anomaly, as well as a summary of other steps used for pre-processing 2005 AVIRIS imagery of Puerto Rico and the U.S. Virgin Islands. The corrected imagery is ready for further analysis and represents a valuable resource for evaluating coral reef conditions at the end of the mass coral bleaching event in 2005. Current analysis is focused on using the imagery to derive water properties, bathymetry, and benthic classification products (Guild et al. 2008). Results from this analysis have been consistent with additional field observations and measurements, thus lending further support to the efficacy of the presented pre-processing scheme.

Acknowledgements

Rob Green and Michael Eastwood (NASA Jet Propulsion Laboratory) provided information throughout this analysis to help us understand the features in the AVIRIS data and their team used their engineering expertise to fix the cause of the stray light. This analysis was supported by the NASA under Grant No. NNH06ZDA001N-IDS issued through the Science Mission Directorate's Earth Science Division. The AVIRIS airborne mission was funded by NASA's Ocean Biology and Biogeochemistry Program. Goodman's work on this project was supported in part by the Bernard M. Gordon Center for Subsurface Sensing and Imaging Systems (Gordon-CenSSIS), under the Engineering Research Centers Program of the National Science Foundation (Award Number EEC-9986821).

References

Carder KL, Reinersman P, Steward RG, Chen RF, Muller-Karger F, Davis CO, Hamilton M (1993) AVIRIS calibration and application in coastal oceanic environments. Remote Sens Environt, 44:205-216.

Chrien TG, Eastwood ML, Sarture CM, Green RO, Porter WM (1991) Current Instrument Status of the Airborne Visible/Infrared Imaging Spectrometer (AVIRIS). Proceedings of the Third Airborne Visible/Infrared Imaging Spectrometer (AVIRIS) Workshop, p. 302-305

Clark RN, Swayze GA (1996) Evolution in imaging spectroscopy analysis and sensor signal-to-noise: an examination of how far we have come. Summaries of the Sixth Annual JPL Airborne Earth Science Workshop. p. 49-53.

Eastwood ML, Green RO, Sarture CM, Chippindale BJ, Chovit CJ, Faust JA, Johnson DL, Monacos SP, Raney JJ (2000) Recent improvements to the AVIRIS sensor: flight season 2000. Proceedings of the Tenth JPL Airborne Earth Science Workshop

Gao B-C, Montes MJ, Ahmad Z, Davis CO (2000) Atmospheric correction algorithm for hyperspectral remote sensing of ocean color from space. Applied Optics 39:887-896

Goodman JA, Ustin SL (2007) Classification of benthic composition in a coral reef environment using spectral unmixing. J Appl Remote Sens 1:011501

Green RO, Boardman J (2000) Exploration of the relationship between information content and signal-to-noise ratio and spatial resolution in aviris spectral data. Proceedings of the Tenth JPL Airborne Earth Science Workshop

Green RO, Chrien TG, Nielsen PJ, Sarture CM, Eng BT, Chovit C, Murray AT, Eastwood ML, Novack HI (1993) Airborne visible/infrared imaging spectrometer (AVIRIS): Recent improvements to the sensor and data facility, SPIE Conf. 1937, Imaging Spectrometry of the Terrestrial Environment: 14-15 April 1993, Orlando, Florida.

Green RO, Pavri B (2000) AVIRIS In-flight calibration experiment, sensitivity analysis, and intraflight stability. Proceedings of the Tenth JPL Airborne Earth Science Workshop

Green RO, Vane G, Conel JE (1988) Determination of in-flight AVIRIS spectral, radiometric, spatial and signal-to-noise characteristics using atmospheric and surface measurements from the vicinity of the rare-earth-bearing carbonatite at Mountain Pass, California. Proceedings of the AVIRIS Performance Evaluation Workshop, JPL Publication 88-38, 162-184

Guild L, Lobitz B, Armstrong R, Gilbes F, Gleason A, Goodman J, Hochberg E, Monaco M, Berthold R (2008) NASA airborne AVIRIS and DCS remote sensing of coral reefs. 11th Int Coral Reef Symposium, Florida USA

Hedley JD, Harborne AR, Mumby PJ (2005) Simple and robust removal of sun glint for mapping shallow-water benthos. Int J Remote Sens 26(10):2107-2112

Hedley JD, Mumby PJ (2003) A remote sensing method for resolving depth and subpixel composition of aquatic benthos. Limnol Oceanogr 48(1):480-488

Hochberg EJ, Andrefouet S, Tyler MR (2003) Sea surface correction of high spatial resolution Ikonos images to improve bottom mapping in near-shore environments. IEEE Trans Geo and Remote Sens 41(7):1724-1729

Mobley CD, Sundman LK, Davis CO, Bowles JH, Downes TV, Leathers RA, Montes MJ, Bisset WP, Kohler DDR, Reid RP, Louchard EM, Gleason A (2005) Interpretation of hyperspectral remote-sensing imagery by spectrum matching and look-up tables. Appl Opt 44:3576-3592

Hochberg EJ, and Atkinson MJ (2000) Spectral discrimination of coral reef benthic communities. Coral Reefs 19:164-171

Hochberg EJ, Atkinson MJ, Andrefouet S (2003) Spectral reflectance of coral reef bottom-types worldwide and implications for coral reef remote sensing. Remote Sens Environ 85:159-173

Montes MJ, Gao B-C, Davis CO (2001) A new algorithm for atmospheric correction of hyperspectral remote sensing data. In Roper W (ed) Geo-Spatial Image and Data Exploitation 2

Montes MJ, Gao B-C, Davis CO (2003) Tafkaa atmospheric correction of hyperspectral data. In Shen SS and Lewis PE (eds) Imaging Spectrometry 9, Proceedings of the SPIE 5159

Sarture, CM, Chrien TG, Green RO, Eastwood ML, Raney JJ, Herrnandez MA (1995) Airborne Visible/Infrared Imaging Spectrometer (AVIRIS) sensor improvements for 1994 and 1995. Summaries of the Fifth Annual JPL Airborne Earth Sciences Workshop, Vol. 1, p. 145-148